The Chemist
Journal of the American Institute of Chemists

Catalysts Immobilized to Magnetic Nanoparticles: Assessment of Particle and Activity Loss During Recycling

Angela, Corbin D. Snavely, Blakely M. Adair-Hudson, and Thaddeus W. Vasicek†

Department of Chemistry, The Citadel, Charleston, SC 29409
†Corresponding author (E-mail: tlevasic@citadel.edu)

Abstract: The immobilization of enzymes to magnetic nanoparticles facilitates the recovery and reuse of the enzyme, which mitigates the financial burden of enzyme use. Particles are typically modified to enhance enzyme immobilization. However, the modification of magnetic nanoparticles alters the magnetic properties of the particles which may diminish the particle recovery and therefore decrease the efficiency of magnetically recycled catalysts. In this work, magnetic nanoparticles were synthesized and modified with varying amounts of an aminosilane. β-Glucosidase, an enzyme relevant for bioethanol production, was immobilized on the particles. The enzyme immobilized particles were subjected to a recycling experiment, where the activity and particle loss during recycling were quantified. The particle loss was ~2% × cycle^{-1} and was not dependent upon the extent of aminosilane modification. The activity loss × cycle^{-1} was ~3% and did not depend on the extent of aminosilane modification but was proportional to the particle loss. The results from this study suggest that increasing the recovery of the magnetic nanoparticles will decrease the loss of recycled enzyme activity.

Key Words: Cellulases, immobilized enzymes, activity loss, magnetic nanoparticles, functional group density

1. Introduction

Enzymes possess many desirable traits as catalysts in the industrial sector. Enzymes have high selectivity, operate in relatively benign solutions, and require low energy input [1]. However, enzymes can account for ~48% of the value of the product [2], which may hinder the use of enzymes in specific sectors. The financial burden of enzyme use is mitigated when the enzymes are recovered and reused for multiple production cycles. Immobilizing enzymes to solid supports enable for the recovery and reuse of the enzymes, thereby reducing their financial impact [3,4].

Nanoparticles (NPs) are routinely used as supports for enzyme immobilization, because they do not suffer from appreciable mass transport limitations, they can be readily modified to facilitate immobilization and they have a high surface area, enabling the immobilization of an abundance of enzyme [1]. Magnetic nanoparticles (MNPs) have the additional benefit of being readily separated from bulk solution by the application of an external magnetic field. This ease of MNP recovery has led to their use in several studies as supports for enzyme immobilization [5-7].

MNPs are modified with agents to introduce functional groups that promote enzyme immobilization. Amines are routinely introduced to MNP surfaces, as the amine can be activated to covalently bind enzymes [8]. Amines can be introduced to the MNP surface by the condensation of 3-aminopropyl triethoxysilane (APTES). The amine density on the MNP is correlated with the APTES concentration used during the modification step, which is pivotal in controlling the enzyme density on the MNP. It is therefore desirable to have MNPs with a high APTES density for the immobilization of large quantities of enzyme.

The financial impact of inactivated enzymes can be minimized when the enzymes maintain high activity throughout subsequent catalytic cycles. Immobilized enzymes will denature during use, which reduces the activity when reused. MNPs with high APTES densities are able to form multiple interactions with the immobilized enzyme and stabilize the enzyme conformation, which hinders inactivation [9,10]. A challenge with APTES modification of MNPs, is that nonmagnetic modifications lower the MNP magnetic susceptibility [11-14] and may reduce the MNP recovery. Incomplete MNP recovery lowers the quantity of catalyst for subsequent production cycles, as immobilized enzyme is lost along with unrecovered MNP. This loss of catalyst would lead to lower subsequent production yields, from reduced catalytic activity when reused.

To the authors' knowledge, there are no reports that simultaneously explore how MNP recovery and recovered enzyme activity are affected by the extent of APTES modification. In this work, the MNP loss and activity loss were studied as a function of APTES modification extent. Specifically, MNPs were modified with different densities of APTES and then β-glucosidase (BGL) was immobilized to the APTES modified MNPs. BGL is an industrially relevant enzyme utilized for the production of bioethanol from cellulose [15]. To assess how the extent of BGL immobilization affects activity and particle recovery, the quantity of BGL used for immobilization was varied to create particles with a low or high BGL loading. The BGL immobilized MNPs were subjected to a recycling experiment where the loss of MNPs and the activity during recycling was studied. Neither the MNP nor activity loss during recycling correlated with the extent of APTES modification. The results of this study indicate that the loss in immobilized BGL activity is primarily caused by incomplete MNP recovery.

2. Experimental Methods

Materials

Water with an electrical resistance of 18 MΩ was used for all experiments. Iron (III) chloride hexahydrate ($FeCl_3 \cdot 6H_2O$) and glutaraldehyde (50%) were purchased from Sigma-Aldrich (St. Louis, MO, USA). Iron (II) chloride tetrahydrate ($FeCl_2 \cdot 4H_2O$), 4-nitrophenyl-β-D-glucopyranoside (*p*NPG), and 3-aminopropyltriethoxysilane (APTES) were purchased from Acros Organics (Geel, Belgium). BGL from almonds, used as received, was purchased from GoldBio (St Louis, MO, USA). Copper (II) sulfate pentahydrate ($CuSO_4 \cdot 5H_2O$), sodium acetate, sodium carbonate, sodium bicarbonate, sodium monohydrogen phosphate, sodium dihydrogen phosphate, ammonium hydroxide (29%), trace-metal grade hydrochloric acid and nitric acid and tetraethyl orthosilicate (TEOS) were purchased from Fisher Scientific (Pittsburgh, PA, USA). Sodium bicinchoninate (BCA), hexylamine, and 4-nitrophenol were purchased from Tokyo Chemical Industry (Portland, OR, USA). The Fe standard was purchased from Spex CertiPrep (Metuchen, NJ, USA).

Preparation and Modification of Iron Oxide Nanoparticles

MNPs were synthesized by the co-precipitation of a 2:1 mole ratio of Fe^{3+} and Fe^{2+} in an aqueous alkaline solution and modified with TEOS, followed by APTES as previously described [16]. In brief, a 47 mL aqueous solution of Fe^{3+} and Fe^{2+} was heated to 80 °C and degassed with N_2 for 30 min. To the iron solution, 2.2 mL of ammonium hydroxide was added dropwise at a rate of 0.5 mL/min and left to stir at 80 °C under N_2 atmosphere for 1 hr. The black precipitate was collected by magnetic decantation, washed twice with degassed H_2O and three times with ethanol.

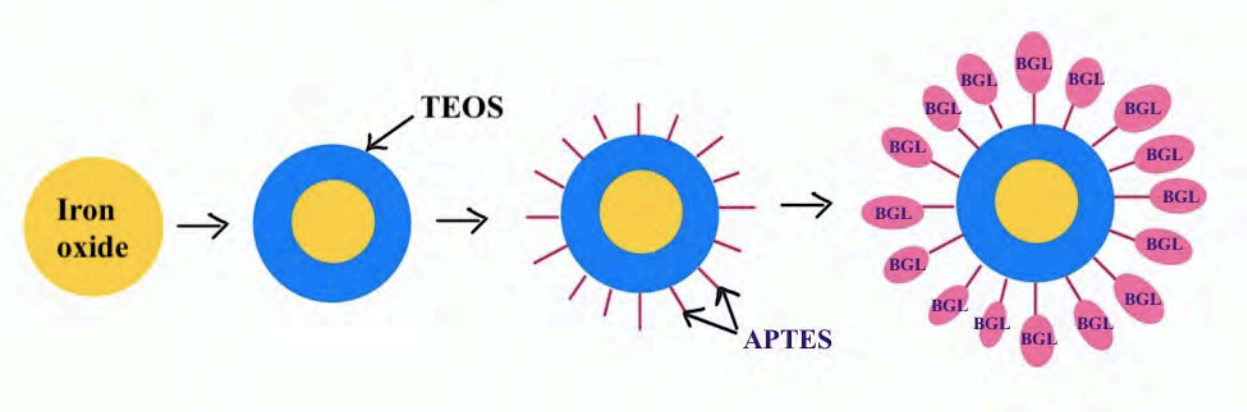

Figure 1. Modification of MNPs. MNPs were initially coated with TEOS, then subsequently modified with varying extents of APTES. Lastly, BGL was immobilized to the APTES modified MNPs.

The prepared MNPs were then modified with TEOS and APTES as displayed in Figure 1. For TEOS modification, 1 mL of the washed MNPs was added to 7.8 mL ethanol, and 0.3 mL of TEOS. The hydrolysis was initiated by the rapid addition of 0.9 mL of 29% ammonium hydroxide and left to react at 350 RPM for 15 hours. The TEOS modified MNPs (MNP-TEOS) were washed three times with ethanol and reconstituted in 15, 30 or 300 mM APTES, hereafter referred to as MNP-TEOS-APTES-15, MNP-TEOS-APTES-30, or MNP-TEOS-APTES-300, respectively. The MNP-TEOS-APTES mixtures were placed on a shaker set at 350 rpm, at room temperature, and allowed to react overnight. The MNP-TEOS-APTES particles were then washed three times in ethanol and dried overnight in a vacuum oven at 60 °C and analyzed using an iS20 ATR-FTIR (Thermo Fisher, Waltham, MA, USA). The MNP-TEOS-APTES were then reacted with glutaraldehyde, which served as a covalent linker between the terminal amine on APTES and primary amines in BGL. A 1 mg/mL MNP solution containing 10 mM phosphate, and 20 mM glutaraldehyde pH 7.4 was created. The solution was placed on a shaker at 350 RPM for 2 hr. After two hours, the MNPs were washed three times into 10 mM acetate pH 5.0 solution containing 0.1 or 1 mg/mL BGL to create particles with a low or high BGL loading, respectively. The BGL-modified MNPs (MNP-TEOS-APTES-BGL) were washed with 10 mM acetate pH 5.0 three times to remove unbound biomolecules. The quantity of immobilized BGL was determined indirectly by mass balance according to equation 1.

$$Immobilization\ Percent\ = \frac{C_i V_i - C_s V_s}{C_i V_i} \times 100 \quad (1)$$

where C_i is the initial concentration of the BGL solution, V_i is the initial volume of solution, C_s is the concentration of the supernatant and V_s is the volume of the supernatant.

Activity Assay and MNP Loss

The BGL activity was quantified using *p*NPG as a model substrate, measuring the 4-nitrophenol produced after 15 min at 37 °C. The MNP-TEOS-APTES-BGLs were gently mixed and diluted to 0.16 mg/mL in 10 mM acetate pH 5.0 to a volume of 750 µL. The kinetic assay was initiated by the addition of 250 µL of 5 mM *p*NPG in 10 mM acetate pH 5.0 to the samples, which were then placed on a shaker at 350 RPM at 37 °C. After 15 min, the MNP-TEOS-APTES-BGLs were magnetically separated for 2 min; the supernatant was removed and split into two aliquots. The 2-minute magnetic separation time was chosen as all the particles were visually observed to be collected within ~20 seconds. One aliquot was added to 200 mM sodium carbonate at a 2:1 volume ratio, and the concentration of 4-nitrophenol determined by measuring the absorbance at 400 nm. The second aliquot was placed in a vacuum oven at 60 °C until dry for analysis by ICP-OES.

Additional cycles of the kinetic assay were performed using the previously used MNP-TEOS-APTES-BGLs. A scheme for the recycling of MNP-TEOS-APTES-BGLs for repeated cycles is shown in Figure 2.

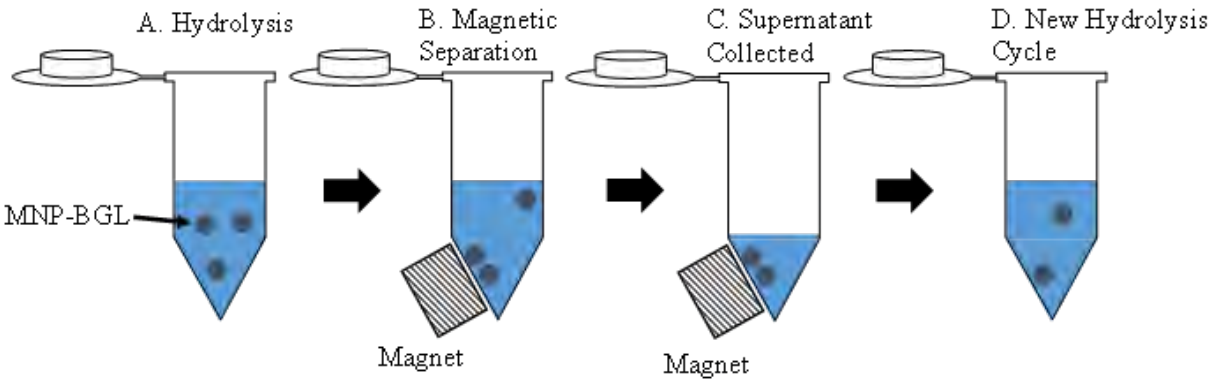

Figure 2. MNP-TEOS-APTES-BGL Recycling Scheme. A) MNP-TEOS-APTES-BGL hydrolyzing cellulose. B) MNP-TEOS-APTES-BGL magnetically separated from bulk. C) Supernatant collected to quantify MNP-TEOS-APTES-BGL loss and BGL activity. D) MNP-TEOS-APTES-BGL washed, fresh substrate added to begin new hydrolysis cycle.

The additional cycles were initiated by washing the MNPs once with 10 mM acetate and adding *p*NPG substrate. The enzyme activity for subsequent cycles was normalized to the activity of the first cycle, and the difference in activity percent for each cycle calculated to determine the activity loss percent.

The quantity of Fe loss during magnetic separation was determined by ICP-OES and assumed to be indicative of MNP-TEOS-APTES-BGLs not recovered during magnetic separation. The dried supernatants were digested in trace metal grade nitric acid at 60 °C for 4 hours. The digested samples were then diluted in 2% nitric acid and analyzed by an Agilent 700 ICP-OES.

3. Results and Discussion

MNP Synthesis and Modification

The magnetic nanoparticles were synthesized by the co-precipitation of Fe^{3+}/Fe^{2+} at a 2:1 mole ratio by the addition of NH_4OH. The synthesis yielded a black precipitate that was readily separated from bulk solution by a handheld neodymium permanent magnet. The handheld neodymium magnet with a 151 pound pull down force was used for the collection of MNPs throughout this study. The synthesized product was modified with TEOS and subsequently APTES. The FTIR spectra for the MNP-TEOS and MNP-TEOS-APTES particles are shown in Figure 3.

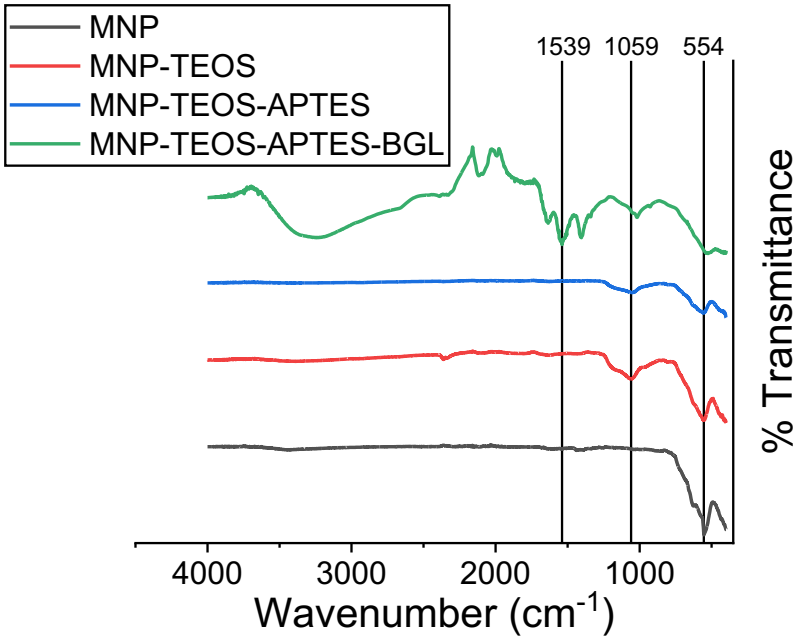

Figure 3. FTIR of MNP (black), MNP-TEOS (red), MNP-TEOS-APTES (blue) and MNP-TEOS-APTES-BGL (green). The spectra are offset for clarity. The peaks at 554, 1059 and 1539 cm^{-1} correspond to the Fe-O from the MNP, the silica from TEOS and the amide bond from BGL, respectively.

The MNPs possessed a peak at 554 cm^{-1}, which is characteristic of the Fe-O bond, and another asymmetric peak at 1059 cm^{-1}, which is indicative of the Si-Fe-Si [17,18]. The MNP-TEOS-APTES particles displayed the same peaks at 554 and 1059 cm^{-1}, however we did not observe a peak corresponding to the terminal amine in APTES at 1530 cm^{-1}. The intensity of the amine peak is proportional to the APTES density on the MNP-TEOS-APTES, and the APTES densities obtained in this study were not significant enough to contribute a prominent FTIR peak. The BGL immobilized particles had a prominent peak at 1539 cm^{-1} which was assigned to the peptide bond from BGL [19].

BGL Immobilization

The MNP-TEOS-APTES particles were reacted with glutaraldehyde and subsequently with BGL. Glutaraldehyde acts as a linker forming covalent bonds between the terminal amine in APTES and a primary amine in BGL [8]. The BGL immobilization percent ranged from 32 to 77% and was greater for particles with a low BGL loading when a 0.1 mg/mL BGL concentration was used for immobilization, as shown in Figure 4.

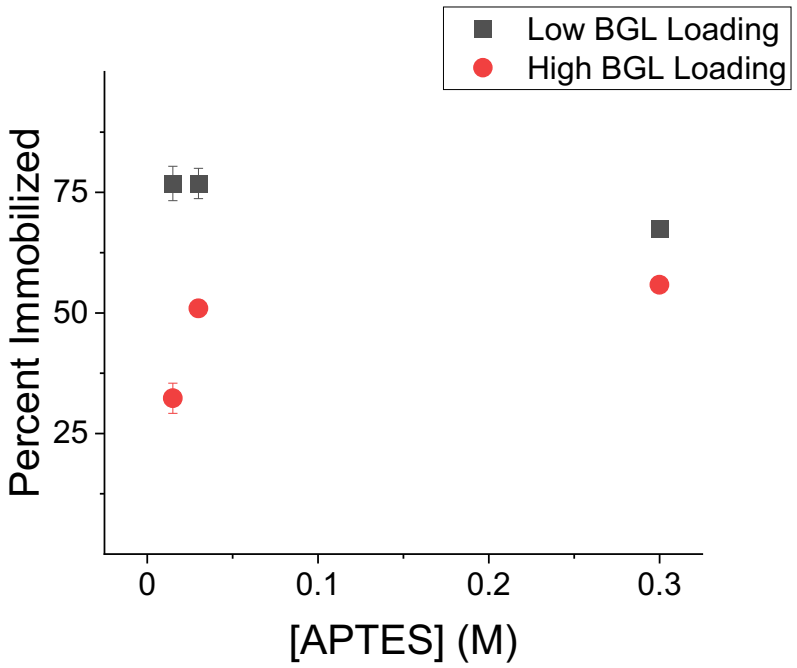

Figure 4. Percent BGL Immobilized on MNP-TEOS-APTES. The [APTES] refers to the [APTES] used for MNP modification. The BGL loading refers to the [BGL] used for immobilization; the low and high loading refer to either a 0.1 or 1 mg/mL BGL solution.

The decrease in immobilization efficiency at the high loading is interpreted initial BGL which attaches to the particle first, sterically hinders subsequent immobilization of adjacent binding sites.

While the presence of APTES was not observed in the IR spectra, the differing BGL immobilization yields between the different APTES concentrations at the high loading suggest that the APTES was present on the MNP-TEOS-APTES particles. Previous work has identified that the APTES concentration used for MNP-TEOS modification is proportional to the APTES density on the MNP-TEOS-APTES particles [16]. While the APTES density on the MNP-TEOS-APTES was not determined in this work, the correlation between the APTES concentration and BGL immobilization yield suggests that the different MNPs have differing APTES densities. At the high loading, MNP-TEOS-APTES-30 and MNP-TEOS-APTES-300 had similar BGL immobilization yields, 51 and 56%, which suggests the particle surface is approaching saturation with BGL.

BGL Activity and MNP Loss

Immobilizing BGL to the MNP-TEOS-APTES permits the capture and reuse of the enzyme. Recovery and reuse of enzymes is practical when immobilization to the particle is efficient, the enzyme maintains activity for subsequent catalytic cycles, and when an abundance of enzyme is immobilized to the MNP. To promote BGL immobilization, the MNP-TEOSs are routinely modified with APTES. However, the APTES modification

of MNP-TEOSs lowers the magnetic susceptibility of the MNP, which may lessen the recovery of the MNP-TEOS-APTES between catalytic cycles. Incomplete recovery of MNP-TEOS-APTES-BGL would reduce the quantity of BGL for subsequent catalytic cycles and be observed as a reduction in activity for future cycles. To assess how the extents of APTES modification altered MNP-TEOS-APTES-BGL recovery, the MNP-TEOS-APTES-BGLs were subjected to a recycling study. The MNP-TEOS-APTES-BGLs were subjected to five catalytic cycles. Between each cycle, the MNP-TEOS-APTES-BGLs were magnetically separated and the supernatants collected. The supernatants were analyzed by ICP-OES to quantify the Fe concentration. The Fe in the supernatants was assumed to be unrecovered particles lost during washing between catalytic cycles.

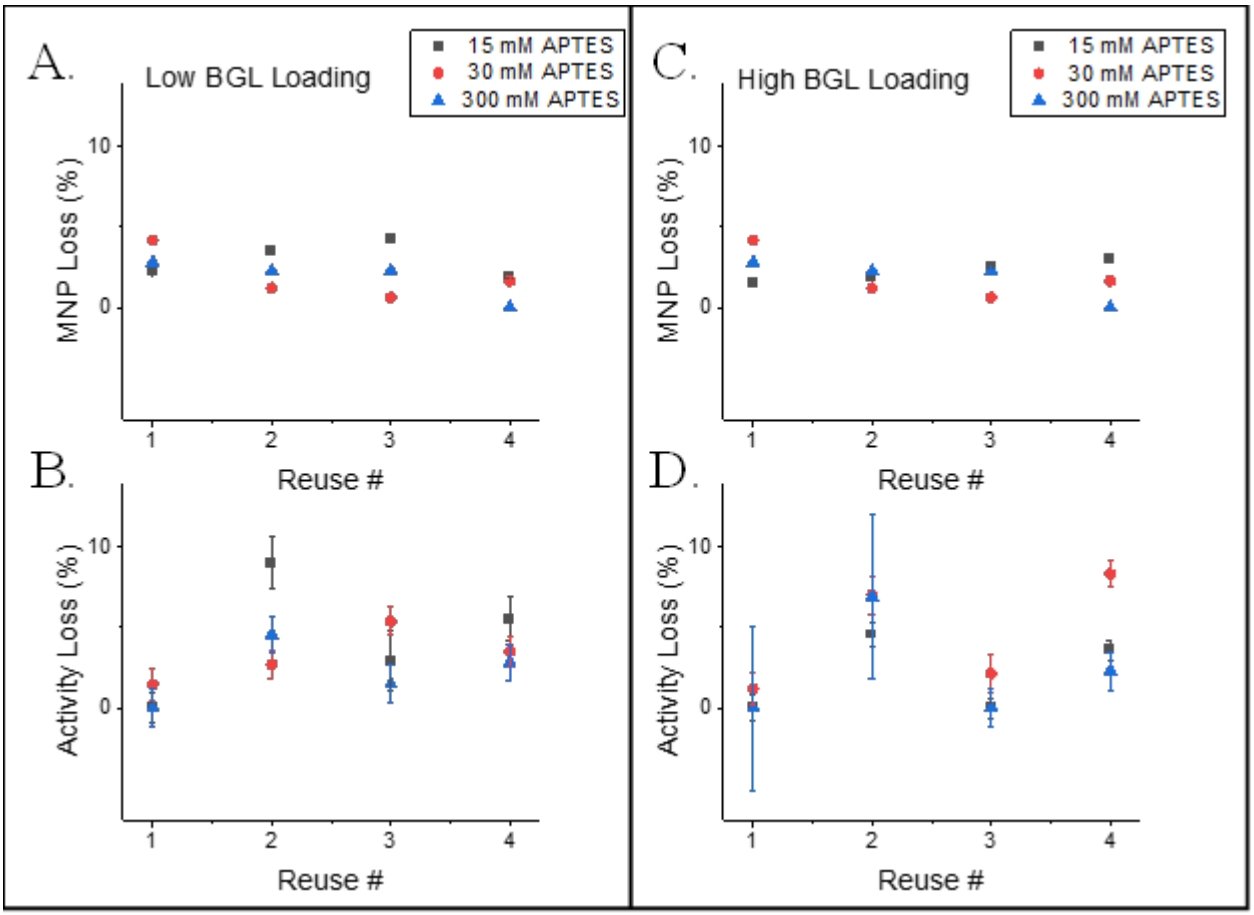

Figure 5. Particle and Activity Loss During Reuse for Particles with a Low BGL Loading (A and B) or a High BGL Loading (C and D). The [APTES] refers to the [APTES] used for MNP modification. BGL activity was measured following a 15 min hydrolysis step at 37 °C in 10 mM acetate buffer pH 5.0.

The particle loss and activity loss per cycle are shown in Figure 5, while the average particle and activity loss are shown in Figure 6.

The average particle loss for each cycle was ~2% relative to the initial Fe concentration. Neither the extent of APTES modification

nor the BGL loading had a significant effect on the particle loss × cycle^{-1} as identified by two-way ANOVAs at the 95% confidence interval. These results were surprising as MNP modification is known to decrease the magnetic susceptibility [12], with the extent of MNP modification correlating to the decrease in magnetization [20]. However, the obtained APTES densities in this work for MNP-TEOS-APTES-15, MNP-TEOS-APTES-30 and MNP-TEOS-APTES-300 may be too similar to cause observable differences in magnetic susceptibility.

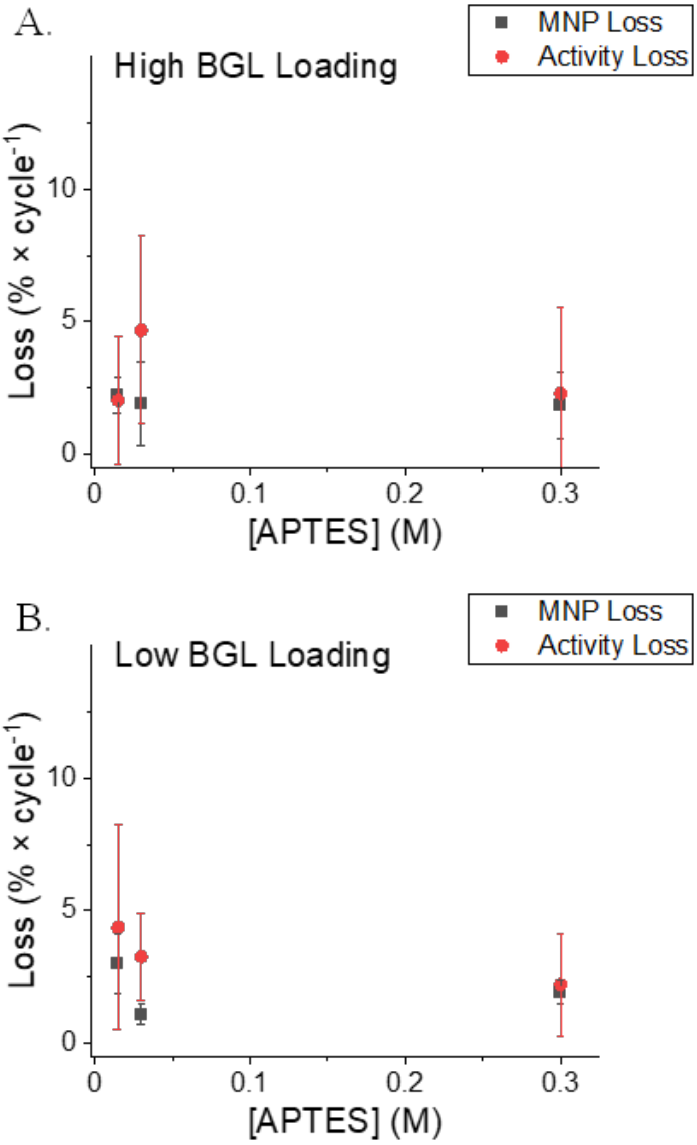

Figure 6. Average Particle Loss (black square) and Average Activity Loss (red circle) During Recycling for High BGL Loading (A) and Low BGL Loading (B).
The [APTES] refers to the [APTES] used for MNP modification. BGL activity was measured following a 15 min hydrolysis step at 37 °C in 10 mM acetate buffer pH 5.0. Avg ± 1 SD.

The immobilized BGL activity decreases upon use due to incomplete particle recovery and enzyme denaturation. The average activity decrease between catalytic cycles ranged from ~0 to 8% per cycle as shown in Figure 6. Neither the extent of APTES modification nor the BGL loading had a significant effect on the activity loss as observed by a two-way ANOVA at the 95% confidence interval. The activity loss per cycle obtained in this study agree with previously reported values of BGL activity loss ranging from ~4 to 6% per cycle [21].

An additional goal of this work was to explore how MNP-TEOS-APTES-BGL loss correlated with activity loss during recycling. The two reasons for activity loss during recycling are loss of the particles and enzyme denaturation. We therefore assumed that the total activity loss during recycling was the sum of the enzyme which denatured and the MNPs which were unrecovered. We analyzed the activity loss and particle loss data using an ANOVA which found no significant difference between the particle and activity loss × $cycle^{-1}$ at the 95% confidence interval. This result suggests that that the loss of particles during magnetic separation is the prime contributor to activity loss during recycling, as unrecovered MNP-TEOS-APTES-BGL cannot participate in subsequent in the hydrolysis of substrate.

The cause(s) of low particle recovery observed in this study could not be elucidated with the present data. However, it is possible that magnetic susceptibility of the MNP-TEOS-APTES-BGLs decreased during use. The particles used in this study were comprised of magnetite, Fe_3O_4. The magnetic susceptibility of magnetite decreases exponentially as the mole ratio of Fe^{3+}:Fe^{2+} deviates from a 2:1 ratio [22], creating a challenge in aqueous applications of MNPs as Fe^{2+} rapidly oxidizes to Fe^{3+} in water [23]. It is possible that oxidation of Fe^{2+} in the particles lowered their recovery during the recycling experiment. Future experiments should quantify the Fe^{3+}/Fe^{2+} ratio in the recovered MNP-TEOS-APTES-BGLs and in the supernatants to identify if Fe oxidation is the cause of MNP-TEOS-APTES-BGL loss.

4. Conclusions

The immobilization of enzymes to MNPs enables the recovery and reuse of BGL. The low protein loading had the highest immobilization efficiency; therefore, immobilization should be performed at the low loading to reduce the financial cost of immobilized BGL. The activity of the recovered enzyme is diminished as the enzyme denatures and due to incomplete recovery MNP. However, low particle recovery is the main determinant in activity loss between catalytic cycles. Further, particle recovery is not affected by the extent of APTES modification nor the protein loading. These results suggest that particle recovery must be optimized to increase the retained activity of recycled catalysts, a pivotal parameter for the industrial use of enzymes immobilized to MNPs.

5. Acknowledgment

Funded by The Citadel Foundation and The Near Center for Climate Studies.

6. References

1. Liese A, Hilterhaus L. Evaluation of immobilized enzymes for industrial applications. *Chem. Soc. Rev.*, 2013, 42(15), 6236-6249. https://doi.org/10.1039/C3CS35511J.
2. Liu G, Zhang J, Bao J. Cost evaluation of cellulase enzyme for industrial-scale cellulosic ethanol production based on rigorous Aspen Plus Modeling. *Bioprocess Biosyst. Eng.*, 2016, 39(1), 133-140. https://doi.org/10.1007/s00449-015-1497-1.
3. Razzaghi M, Homaei A, Vianello F, Azad T, Sharma T, Nadda AK, Stevanato R, Bilal M, Iqbal HMN. Industrial applications of immobilized nano-biocatalysts. *Bioprocess Biosyst. Eng.*, 2022, 45(2), 237-256. https://doi.org/10.1007/s00449-021-02647-y.
4. DiCosimo R, McAuliffe J, Poulose AJ, Bohlmann G. Industrial use of immobilized enzymes. *Chem. Soc. Rev.*, 2013, 42(15), 6437-6474. https://doi.org/10.1039/C3CS35506C.
5. Khoshnevisan K, Poorakbar E, Baharifar H, Barkhi M. Recent advances of cellulase immobilization onto magnetic nanoparticles: An update review. *Magnetochemistry*, 2019, 5(2). https://doi.org/10.3390/magnetochemistry5020036.
6. Melo RLF, Sales MB, de Castro Bizerra V, de Sousa Junior PG, Cavalcante ALG, Freire TM, Neto FS, Bilal M, Jesionowski T, Soares JM, Fechine PBA, Dos Santos JCS. Recent applications and future prospects of magnetic biocatalysts. *Int. J. Biol. Macromol.*, 2023, 253 (Pt 3), 126709. https://doi.org/10.1016/j.ijbiomac.2023.126709.
7. Khoshnevisan K, Vakhshiteh F, Barkhi M, Baharifar H, Poor-Akbar E, Zari N, Stamatis H, Bordbar A-K. Immobilization of cellulase enzyme onto magnetic nanoparticles: Applications and recent advances. *Mol. Catal.*, 2017, 442, 66-73. https://doi.org/10.1016/j.mcat.2017.09.006.
8. Vandenberg E, Elwing H, Askendal A, Lundström I. Protein immobilization of 3-aminopropyl triethoxy silaneglutaraldehyde surfaces: Characterization by detergent washing. *J. Colloid Interface Sci.*, 1991, 143(2), 327-335. https://doi.org/10.1016/0021-9797(91)90266-B.
9. Bilal M, Asgher M, Cheng H, Yan Y, Iqbal HMN. Multi-point enzyme immobilization, surface chemistry, and novel platforms: A paradigm shift in biocatalyst design. *Crit. Rev. Biotechnol.*, 2019, 39(2), 202-219.

https://doi.org/10.1080/07388551.2018.1531822.
10. Adriano WS, Filho EHC, Silva JA, Gonçalves LRB. Optimization of penicillin G acylase multipoint immobilization on to glutaraldehyde-chitosan beads. *Biotechnol. Appl. Biochem.*, 2005, 41(3), 201-207. https://doi.org/10.1042/BA20040061
11. Banaei M, Salami-Kalajahi MA. Grafting to approach to synthesize low cytotoxic poly(aminoamide)-dendrimer-grafted Fe_3O_4 magnetic nanoparticles. *Adv. Polym. Technol.*, 2018, 37(3), 943-948. https://doi.org/10.1002/adv.21741.
12. Ghazanfari MR, Kashefi M, Shams SF, Jaafari MR. Perspective of Fe_3O_4 nanoparticles role in biomedical applications. *Biochem. Res. Int.*, 2016, 2016, 7840161. https://doi.org/10.1155/2016/7840161.
13. Dhavale RP, Waifalkar PP, Sharma A, Dhavale RP, Sahoo SC, Kollu P, Chougale AD, Zahn DRT, Salvan G, Patil PS, Patil PB. Monolayer grafting of aminosilane on magnetic nanoparticles: An efficient approach for targeted drug delivery system. *J. Colloid Interface Sci.*, 2018, 529, 415-425. https://doi.org/10.1016/j.jcis.2018.06.006.
14. Yuan Y, Rende D, Altan CL, Bucak S, Ozisik R, Borca-Tasciuc D-A. Effect of surface modification on magnetization of iron oxide nanoparticle colloids. *Langmuir ACS J. Surf. Colloids*, 2012, 28(36), 13051-13059. https://doi.org/10.1021/la3022479.
15. Singh G, Verma AK, Kumar V. Catalytic properties, functional attributes and industrial applications of β-glucosidases. *3 Biotech*, 2016, 6(1), 3. https://doi.org/10.1007/s13205-015-0328-z.
16. Vasicek TW, Guillermo S, Swofford DR, Durchman J, Jenkins SV. β-Glucosidase immobilized on magnetic nanoparticles: Controlling biomolecule footprint and particle functional group density to navigate the activity-stability tradeoff. *ACS Appl. Bio Mater.*, 2022, 5(11), 5347-5355. https://doi.org/10.1021/acsabm.2c00735.
17. Ma M, Zhang Y, Yu W, Shen H, Zhang H, Gu N. Preparation and characterization of magnetite nanoparticles coated by amino silane. *Colloids Surf., A*, 2003, 212(2), 219-226. https://doi.org/10.1016/S0927-7757(02)00305-9.
18. Shahbazi R, Babazadeh M, Afzali E. Surface modification of silica-coated on the magnetic nanoparticles with covalently immobilized between imidazolium cation and silane groups for potential application as a green catalyst. *MOJ Bioorg. Org. Chem.*, 2018, 2. https://doi.org/10.15406/mojboc.2018.02.00048.
19. Barth A. Infrared spectroscopy of proteins. *Biochim. Biophys. Acta, Bioenerg.*, 2007, 1767(9), 1073-1101. https://doi.org/10.1016/j.bbabio.2007.06.004.
20. Digigow RG, Dechézelles J-F, Dietsch H, Geissbühler I, Vanhecke D, Geers C, Hirt AM, Rothen-Rutishauser B, Petri-Fink A. Preparation and characterization of functional silica hybrid magnetic nanoparticles. *J. Magn. Magn. Mater.*, 2014, 362, 72-79.

https://doi.org/10.1016/j.jmmm.2014.03.026.
21. Park HJ, Driscoll AJ, Johnson PA. The development and evaluation of β-glucosidase immobilized magnetic nanoparticles as recoverable biocatalysts. *Biochem. Eng. J.*, 2018, 133, 66-73. https://doi.org/10.1016/j.bej.2018.01.017.
22. Schwaminger SP, Bauer D, Fraga-García P, Wagner FE, Berensmeier S. Oxidation of magnetite nanoparticles: Impact on surface and crystal properties. *CrystEngComm*, 2017, 19(2), 246-255. https://doi.org/10.1039/C6CE02421A.
23. Demangeat E, Pédrot M, Dia A, Bouhnik-le-Coz M, Grasset F, Hanna K, Kamagate M, Cabello-Hurtado F. Colloidal and chemical stabilities of iron oxide nanoparticles in aqueous solutions: The interplay of structural, chemical and environmental drivers. *Environ. Sci.: Nano*, 2018, 5(4), 992-1001. https://doi.org/10.1039/C7EN01159H.